AAPS PharmSciTech, Vol. 12, No. 4, December 2011 (© 2011)
DOI: 10.1208/s12249-011-9686-y

Research Article

Understanding the Tendency of Amorphous Solid Dispersions to Undergo Amorphous–Amorphous Phase Separation in the Presence of Absorbed Moisture

Alfred C. F. Rumondor,[1] Håkan Wikström,[2] Bernard Van Eerdenbrugh,[1,3] and Lynne S. Taylor[1,4]

Received 23 May 2011; accepted 2 September 2011; published online 17 September 2011

Abstract. Formulation of an amorphous solid dispersion (ASD) is one of the methods commonly considered to increase the bioavailability of a poorly water-soluble small-molecule active pharmaceutical ingredient (API). However, many factors have to be considered in designing an API–polymer system, including any potential changes to the physical stability of the API. In this study, the tendency of ASD systems containing a poorly water-soluble API and a polymer to undergo amorphous–amorphous phase separation was evaluated following exposure to moisture at increasing relative humidity. Infrared spectroscopy was used as the primary method to investigate the phase behavior of the systems. In general, it was observed that stronger drug–polymer interactions, low-ASD hygroscopicity, and a less hydrophobic API led to the formation of systems resistant to moisture-induced amorphous–amorphous phase separation. Orthogonal partial least squares analysis provided further insight into the systems, confirming the importance of the aforementioned properties. In order to design a more physically stable ASD that is resistant to moisture-induced amorphous–amorphous phase separation, it is important to consider the interplay between these properties.

KEY WORDS: amorphous; amorphous solid dispersion; partial least squares (PLS); sorbed moisture.

INTRODUCTION

Many small-molecule active pharmaceutical ingredients (APIs) in development are poorly soluble in water, which may subsequently lead to limited bioavailability. In order to enable the delivery of these compounds in tablet or capsule forms, different strategies are commonly used to increase their solubility. One such strategy, delivery of the API in the amorphous form (pure or as a mixture with another component) presents an attractive option, due to the potential for large increases in apparent solubility (1). However, in order to ensure that the performance benefits resulting from increased solubility are realized, conversion of an amorphous API to a thermodynamically more stable crystalline form must be inhibited. Inhibition of API crystallization from the amorphous form must be prevented throughout the lifetime of the intended pharmaceutical product. Thus, the pharmaceutical product should be designed to be robust, with no changes to its chemical or physical properties over a desirable time frame.

The phase behavior of an amorphous system can be affected by different factors. One factor in particular, the absorption of moisture, has been shown to accelerate crystallization of amorphous APIs in pure form as well as when mixed with other ingredients (2–4). For binary systems, it has been demonstrated that the absorption of moisture can lead to the formation of regions with different API–polymer concentrations from the corresponding one-phase amorphous system (where the API and the polymer were originally mixed at the molecular level) (5). Here, the absorption of moisture induces amorphous–amorphous phase separation. This phenomenon has been shown to occur in certain amorphous dispersions (5), but not in others (6,7). Important factors dictating the phase behavior on exposure to moisture are thought to include the strength of API–polymer interactions (7,8) as well as the hygroscopicity of the binary system (6) (which in turn depends on the hygroscopicity of the individual components as well as the strength of their interactions (9)). The objective of the current study was to probe further the effect of moisture on API–polymer miscibility by investigating additional model systems, supplemented by the application of chemometric data analysis methods to better understand the observed behavior.

The model APIs selected for this study differed in their ability to act as hydrogen-bond donors, such that the effect of varying the strength of the API–polymer interaction on the propensity of the system to undergo moisture induced amorphous–amorphous phase separation could be probed. Polyvinylpyrrolidone (PVP) was used as the model polymer

[1] Department of Industrial and Physical Pharmacy, College of Pharmacy, Purdue University, West Lafayette, Indiana 47907 USA.
[2] Pharmaceutical Development, AstraZeneca Pharmaceuticals, Mölndal, Sweden.
[3] Laboratory for Pharmacotechnology and Biopharmacy, K. U. Leuven, Gasthuisberg O&N2, Herestraat 49, Box 921, 3000 Leuven, Belgium.
[4] To whom correspondence should be addressed. (e-mail: lstaylor@purdue.edu)

and the phase behavior of the API–polymer dispersions was assessed immediately after production as well as following exposure to increasing storage relative humidity. A discriminant analysis model was constructed in order to identify the factors most important in determining the resistance of an amorphous molecular-level solid dispersion system (ASD for short) containing a hydrophobic API towards amorphous–amorphous phase separation in the presence of absorbed moisture.

MATERIALS AND METHODS

Materials

Dichloromethane and isopropanol (ChromAR grade) and chloroform (AR grade) were obtained from Mallinckrodt Baker, Inc., Paris, Kentucky, USA, while ethanol (200 proof) was obtained from Aaper Alcohol and Chemical Co., Shelbyville, Kentucky, USA. Poly(vinyl pyrrolidone) (PVP) K29-32, indoprofen, nilutamide, probucol, and clofoctol were purchased from Sigma-Aldrich Co., St. Louis, Missouri, USA and loratadine was purchased from Attix Pharmachem, Toronto, Ontario, Canada. Prior to use, PVP was dried in a desiccator over powdered phosphorus pentoxide for at least 1 week. The chemical structures of the different model compounds used in this study are presented in Fig. 1.

Methods

Infrared Spectroscopy

Binary mixtures of the model APIs and PVP were prepared at different weight ratios and dissolved in a common solvent. For clofoctol–PVP, the solvent used was a 1:1 *w*/*w* mixture of dichloromethane and ethanol, while for probucol–PVP, pure ethanol was used. For loratadine and indoprofen–PVP systems, chloroform was used, and for nilutamide–PVP, the solvent was isopropanol. All mixtures were visually inspected to confirm that the API and the polymer were fully dissolved, and the systems formed uniform one-phase solutions.

A few drops of the solution were then placed on ZnS or KRS-5 substrates, which were immediately rotated on a KW-4A two-stage spin coater (Chemat Technology, Northridge, California, USA) at 500/2,500 rpm for 18 and 30 s, respectively. Immediately after spin-coating, the substrates were transferred onto a hot plate set to 90°C for at least a minute to remove any residual solvents. Infrared spectra of the resulting thin films were obtained in absorbance mode using a Bio-Rad FTS 6,000 spectrophotometer (Bio-Rad Laboratories, Hercules, California, USA) equipped with globar infrared source, KBr beamsplitter, and DTGS detector. The scan range was set from 500 to 4,000 cm^{-1} with 4 cm^{-1} resolution, and 128 scans were co-added. Care was taken to ensure that the absorbance intensity of the spectral region of interest was between 0.6 and 1.0. During infrared measurements, the spin-coated samples and the sample compartment of the spectrophotometer were flushed with dry air (<10% relative humidity (RH)) in order to minimize interference from absorbed and gas-phase moisture.

Spin-coated thin film samples of each system at a particular API-to-polymer ratio were also prepared by spin coating and stored in desiccators maintained at 54%, 75%, 84%, or 94% RH using saturated solutions of $Mg(NO_3)_2$, NaCl, KCl, and KNO_3 salts, respectively. Periodically, the samples were removed from the desiccators and dried by flushing with dry air (RH<10%) *in situ* until no changes in the OH region of the spectra was observed. The infrared spectra of the dried samples were then collected. Rigorous drying of the solid dispersion samples before analysis was performed to ensure that absorbed moisture would not mask changes in the extent of API–polymer interactions.

Reference spectra of the amorphous form of the APIs and pure PVP were collected using the aforementioned spin-coating technique, while reference spectra of the crystalline APIs as received were obtained using a Golden Gate™ MII

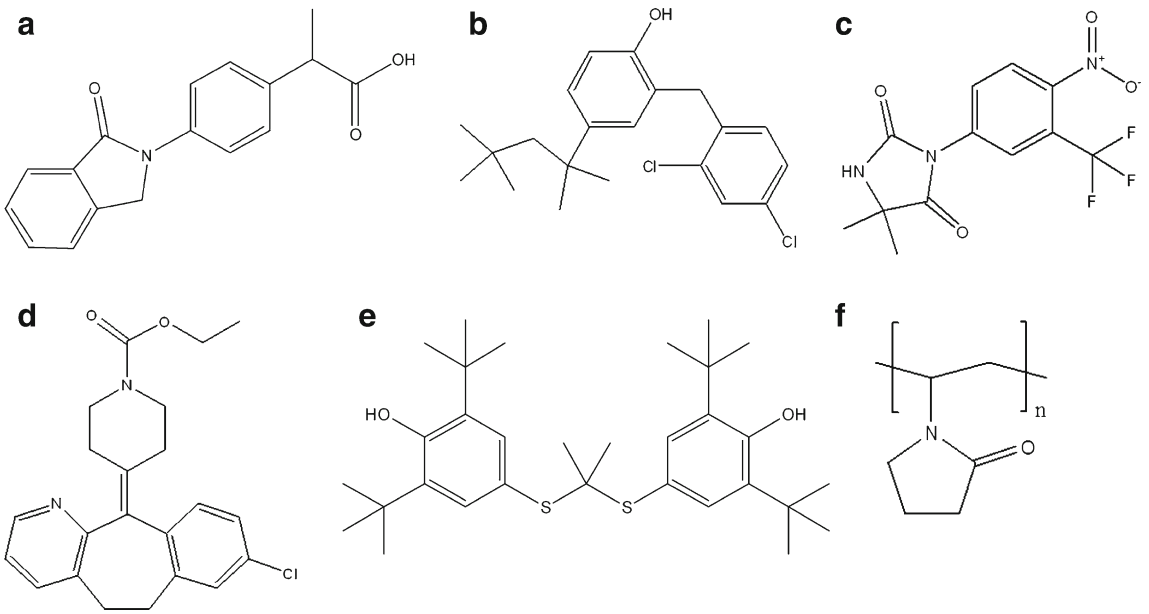

Fig. 1. The chemical structures of **a** indoprofen, **b** clofoctol, **c** nilutamide, **d** loratadine and **e** probucol, and **f** the repeating unit of PVP

attenuated total reflectance unit with diamond top plate (Specac Inc., Woodstock, Georgia, USA).

Powder X-ray Diffraction

To confirm the amorphous nature of the samples, as inferred from the infrared spectroscopic studies, powder X-ray diffraction (PXRD) studies were carried out on selected samples. Binary mixtures of all the model APIs and PVP (total weight 250–500 mg) were prepared in bulk at 50:50 weight ratios. Subsequently, the mixtures were dissolved in a common solvent, using the solvent systems specified above. All mixtures were visually inspected to confirm that the drug and polymer were completely dissolved, and the systems formed uniform one-phase solutions. The solvent was then removed using a rotary evaporator apparatus (Rotavapor R, Büchi Labortechnik AG, Flawil, Switzerland). Subsequently, the resulting powder was transferred into an aluminum PXRD sample holder. The latter was briefly placed on a hot plate to remove any residual solvents. PXRD data were obtained using CuK_{α} radiation with a Shimadzu XRD-6,000 powder diffractometer (Shimadzu Scientific Instruments, Columbia, Maryland, USA) operating at 40 kV and 30 mV. The X-ray measurements were conducted in Bragg-Brentano mode using a scan range of 5–35°2θ, a scan rate of 4°2θ/min with a step size of 0.04°. The [111] peak of a Si standard was used as an external standard. PXRD measurements were collected immediately after production and following storage at 84% RH (saturated KCl solution) in a desiccator for 18 and 42 h.

Chemometrics Analysis

Orthogonal projections to latent structures discriminant analysis (OPLS-DA) was performed using SIMCA-P+ v.12.0.1 software (Umetrics AB, Umeå, Sweden). OPLS-DA is a discriminant analysis technique where within-class variation is captured in orthogonal components, while the between-class differences are captured in the predictive component (10). The additional orthogonal projections are often used to assist interpretation of discriminant analysis models.

RESULTS

Miscibility of API–Polymer Systems in the Absence of Moisture

Spin-coated films of the drug–polymer systems were transparent suggesting the formation of amorphous films. PXRD of dispersions prepared in bulk gave a halo pattern, typical of amorphous systems (data not shown). API–polymer miscibility for the model systems was initially investigated in the absence of moisture. In ASDs, changes are observed in the infrared spectra of the binary systems that cannot be attributed to variations in the composition of the samples (11). These changes are especially apparent in the spectral regions arising from chemical moieties involved in API–polymer hydrogen-bonding interactions.

Clofoctol and probucol have OH-type hydrogen-bond donors, and no carbonyl moieties (see Fig. 1). PVP, on the other hand, has carbonyl hydrogen-bond acceptor groups, and no hydrogen-bond donors. Thus, in ASDs comprised of these API–polymer combinations, changes can be observed in the regions of the infrared spectra attributed to the carbonyl and OH moieties. In the clofoctol–PVP system, evidence of API–polymer specific interactions (Fig. 2) can be observed as a red shift of the PVP carbonyl peak from 1,682 to 1,663 cm^{-1}. In addition, the peak centered at 3,365 cm^{-1}, assigned to the free OH moiety of clofoctol, shifts to 3,263 cm^{-1}, and broadens in the well-mixed binary systems, providing further evidence of API–polymer hydrogen bonding (results not shown). In probucol–PVP, a similar red shift was also observed in the PVP carbonyl peak from 1,682 to 1,663 cm^{-1} (data not shown), which is consistent with the formation API–polymer hydrogen bonds for this system as reported in literature (12).

In the indoprofen–PVP system, changes in the infrared spectra due to API–polymer specific interactions can be observed in the carbonyl region, shown in Fig. 3, as previously reported for indomethacin–PVP and ketoprofen–PVP systems (7,13). In order to ascertain the presence of API–polymer interactions in the ASDs, the theoretical spectra of physical mixtures containing pure amorphous indoprofen and PVP were calculated based on the number of C–C bonds in the molecule (the complete spectral calculation details are explained in reference (7)). The results clearly show that the spectra of indoprofen–PVP solid dispersion samples cannot be constructed from the spectra of the pure amorphous components, for example, as shown

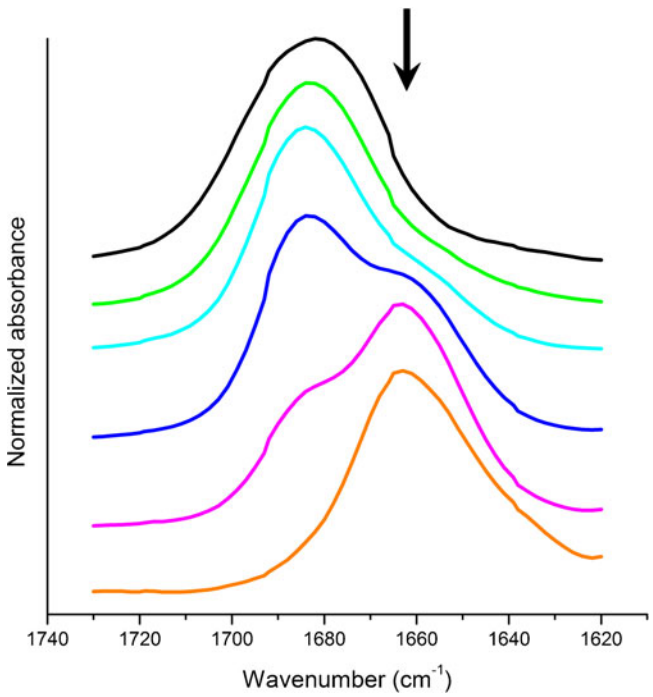

Fig. 2. Infrared spectra of the carbonyl region of clofoctol–PVP solid dispersion samples containing (top to bottom): (*black*) 100, (*green*) 90, (*cyan*) 70, (*blue*) 50, (*magenta*) 30, and (*orange*) 10% PVP (*w/w*). Pure clofoctol does not have significant infrared absorption in this region. The arrow shows the development of a new peak arising from the PVP carbonyl group hydrogen bonded to the drug. The spectra of probucol–PVP systems show peaks at the same locations, and are not shown here

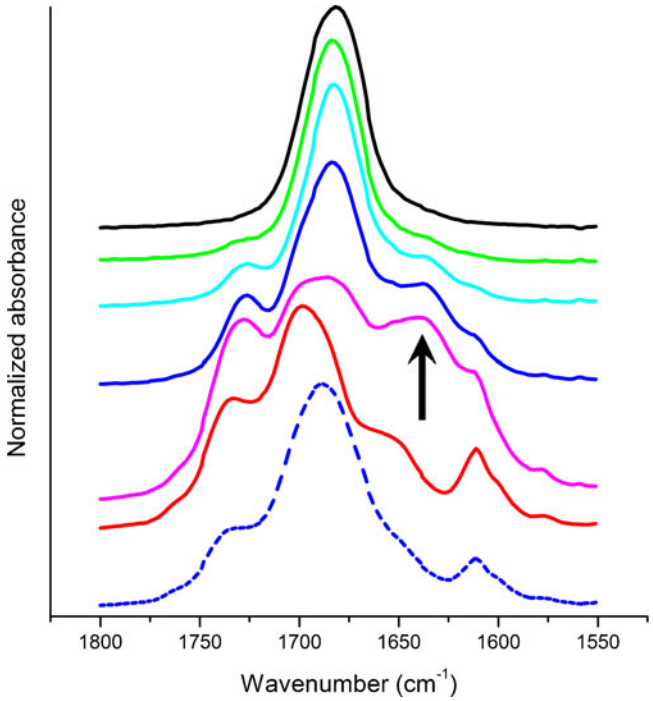

Fig. 3. Infrared spectra of the carbonyl region of indoprofen–PVP solid dispersion samples containing (*top to bottom*): (*solid black*) 100, (*solid green*) 90, (*solid cyan*) 70, (*solid blue*) 50, (*solid magenta*) 30, and (*solid red*) 0% PVP (*w/w*). The calculated spectrum of a physical mixture containing 50% pure amorphous API and pure PVP (*dashed blue*) is also included for comparison. The arrow shows the development of a new peak arising from the PVP carbonyl group hydrogen bonded to the drug

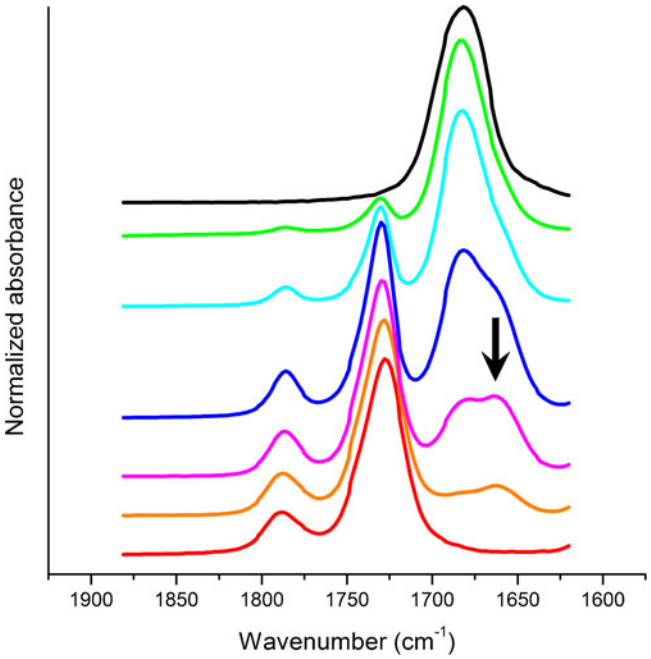

Fig. 4. Infrared spectra of the carbonyl region of nilutamide–PVP solid dispersion samples containing (*top to bottom*): (*black*) 100, (*green*) 90, (*cyan*) 70, (*blue*) 50, (*magenta*) 30, (*orange*) 10, and (*red*) 0% PVP (*w/w*). The arrow shows the development of a new peak arising from the PVP carbonyl group hydrogen bonded to the drug

with the sample containing 50% PVP (*w/w*) (see Fig. 3). When the PVP concentration in the ASD system was reduced from 100% to 70% *w/w*, a decrease in the relative intensity of the free PVP carbonyl peak, centered at 1,682 cm^{-1}, was observed, along with the development of a shoulder at 1,641 cm^{-1}. The former peak is assigned to the carbonyl peak of non-hydrogen-bonded PVP, while the latter is attributed to the carbonyl peak of PVP when hydrogen bonded to the COOH moiety in indoprofen.

Two peaks can be observed in the carbonyl region of the infrared spectrum of amorphous nilutamide (Fig. 4), centered at 1,787 and 1,729 cm^{-1}, respectively, which can be attributed to the two carbonyl moieties of the molecule. When nilutamide was intimately mixed with PVP as in the ASDs, a shoulder developed at 1,663 cm^{-1}. This peak is assigned to the carbonyl peak of PVP when hydrogen bonded to the NH moiety of the API. No change was observed in the position of the nilutamide carbonyl peaks.

Loratadine does not have a typical hydrogen-bond donor moiety although close examination of loratadine crystal structure (Cambridge Structural Database (14) reference code BEQGIN) shows the formation of weak hydrogen bonds between the carbonyl group and an aromatic proton. In loratadine–PVP ASDs, no hydrogen bonds are anticipated between the API and the polymer, which resulted in more subtle spectroscopic changes as shown in Fig. 5. The infrared peak attributed to the carbonyl moiety in pure amorphous loratadine is centered at 1,698 cm^{-1}, while the peak for pure PVP is centered at 1,682 cm^{-1}. In the ASDs, the two peaks are merged together, forming one broad peak centered between these two peaks. The shape of the combined peaks

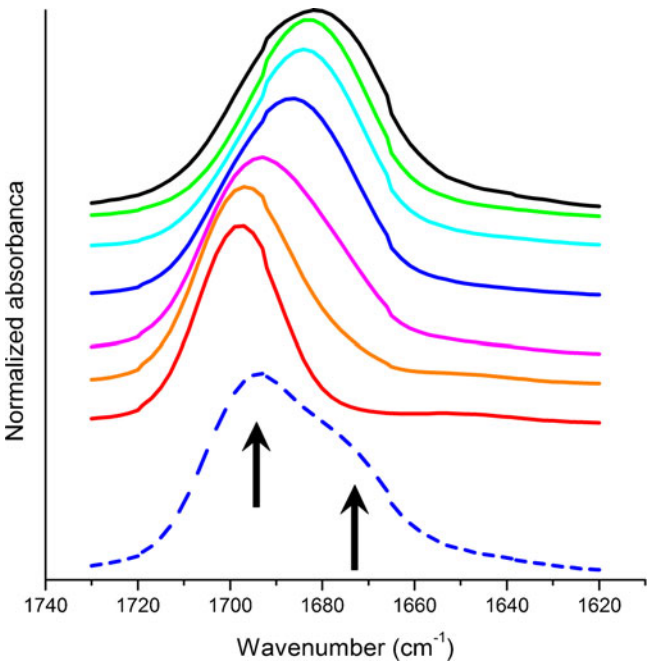

Fig. 5. Infrared spectra of the carbonyl region of loratadine–PVP solid dispersion samples containing (*top to bottom*): (*black*) 100, (*green*) 90, (*cyan*) 70, (*blue*) 50, (*magenta*) 30, (*orange*) 10, and (*red*) 0% PVP (*w/w*). The calculated spectrum of a physical mixture containing 50% pure amorphous API and pure PVP (*dashed blue*) is also included for comparison

in the ASDs is different from the theoretically calculated spectra of loratadine–PVP physical mixtures, as indicated in Fig. 5. This observation indicated the presence of intimate mixing between the API and the polymer in the ASDs.

Miscibility of API-Polymer Systems in the Presence of Absorbed Moisture

When an ASD comprised of a hydrophobic API and a polymer is exposed to moisture, API–polymer miscibility in the system can be adversely impacted. Specifically, if amorphous–amorphous phase separation occurs in a given system, polymer-rich and API-rich amorphous domains will be formed (5–7). Such changes will be reflected in the infrared spectra of the samples as an enhancement in features attributable to pure amorphous API or pure PVP at the expense of spectral features attributable to API–polymer interactions.

The miscibility of the different API–polymer systems studied was assessed by obtaining the infrared spectra of the model systems before and after storage at increasing relative humidity. For these samples, it was important to differentiate spectroscopic changes due to amorphous–amorphous phase separation from those due to crystallization. This was done by carefully comparing the resultant spectra to the reference crystalline and amorphous spectra. In addition, PXRD studies of select dispersions following exposure to 84% RH for up to 42 h (data not shown) were undertaken; all samples remained amorphous following these storage conditions, in good agreement with the results of the IR studies shown in Table I. In clofoctol–PVP systems, when the ASD sample containing 50% (*w*/*w*) PVP was exposed to moisture at 54% RH, a reduction in the intensity of the peak centered at 1,663 cm^{-1} was observed relative to the peak centered at 1,682 cm^{-1} (see Fig. 6). Since the former is assigned to the carbonyl peak of PVP when hydrogen bonded to the API, a reduction in its relative intensity is consistent with the formation of more free PVP carbonyl groups, indicative of amorphous–amorphous phase separation in the system. As the storage RH was increased to 75%, 84%, and 94%, the intensity of the peak attributed to API–polymer interactions kept decreasing; however, overlap with the pure PVP peak resulted in peak shifts towards the peak centered at 1,682 cm^{-1}. The absence of crystalline clofoctol in the system was verified visually as well as through the absence of peaks characteristic of crystalline clofoctol found in the infrared spectra at 854 and 1,238 cm^{-1}. Similar spectral changes, to varying extents, were also observed in samples containing 70% (see Fig. 6, bottom two spectra) and 90% PVP (results not shown). However, these changes were not observed in samples containing 30% (see Fig. 6, top two spectra) and 10% PVP (results not shown). For these samples, after exposure of the samples to moisture at increasing RHs up to 94% and subsequent drying, the infrared spectra of the samples were identical to the spectra of the samples immediately after preparation.

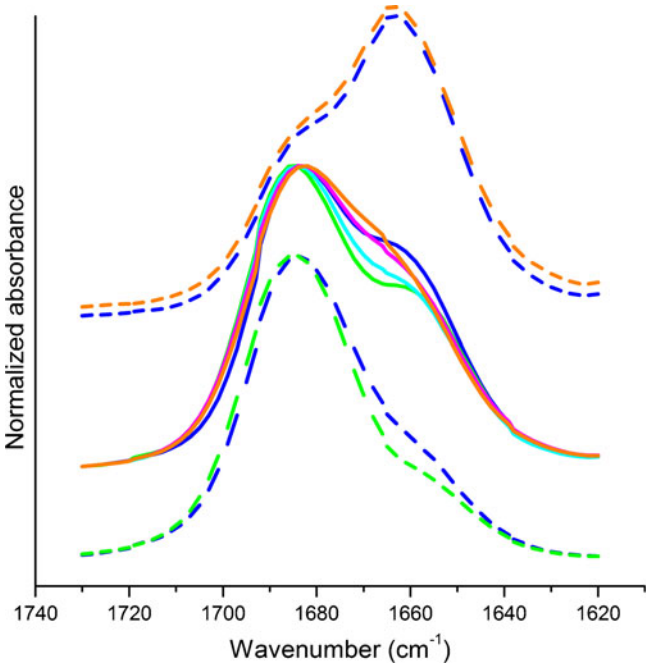

Fig. 6. Infrared spectra of the carbonyl region of clofoctol–PVP solid dispersion samples containing 30% (*two dashed lines on top*), 50% (*middle five solid lines*), and 70% (*two dashed lines at the bottom*) PVP. In each series, the spectra are color coded as follows: (*blue*) initial spectrum, and following storage at (*green*) 54, (*cyan*) 75, (*magenta*) 84, and (*orange*) 94% relative humidity with subsequent drying

In the probucol–PVP system, exposure of the sample containing 50% (*w*/*w*) PVP to moisture at increasing RH also resulted in a gradual reduction in the relative intensity of the peak centered at 1,663 cm^{-1} (appears as a shoulder due to peak overlap) compared to the peak centered at 1,682 cm^{-1} (Fig. 7). Similar changes were observed in samples containing 70% and 90% PVP. The changes in the infrared spectral feature attributed to API–polymer specific interactions for the sample containing 30% PVP were much smaller in extent, and not observed at all in the sample containing 10% PVP.

Table I. Phase Behavior of ASD Samples Containing a Hydrophobic API and PVP When Exposed to Moisture at 22°C and Different Relative Humidity

PVP % (*w*/*w*)	Clofoctol–PVP	Probucol–PVP	Indoprofen–PVP	Nilutamide–PVP	Loratadine–PVP
10	NC	NC	API crystallization at 54% RH	AAPS	AAPS
30	NC	AAPS (slight)	AAPS at 54% RH, API crystallization at 75% RH	AAPS	AAPS
50	AAPS	AAPS	AAPS at 54% RH, API crystallization at 84% RH	AAPS	AAPS
70	AAPS	AAPS	AAPS	AAPS	AAPS
90	AAPS	AAPS	AAPS	AAPS	AAPS

NC no changes in the spectra of ASD samples following storage at 94% RH
AAPS evidence of amorphous–amorphous phase separation was observed following storage at increasing RH

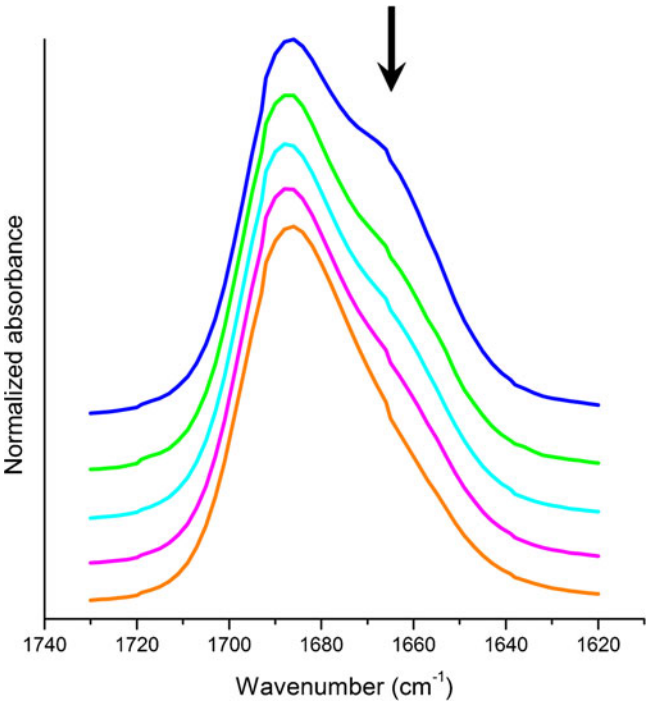

Fig. 7. Infrared spectra of the carbonyl region of probucol–PVP solid dispersion samples containing (*top to bottom*): (*blue*) 50% API immediately after formation, and following storage at (*green*) 54, (*cyan*) 75, (*magenta*) 84, and (*orange*) 94% relative humidity and subsequent drying

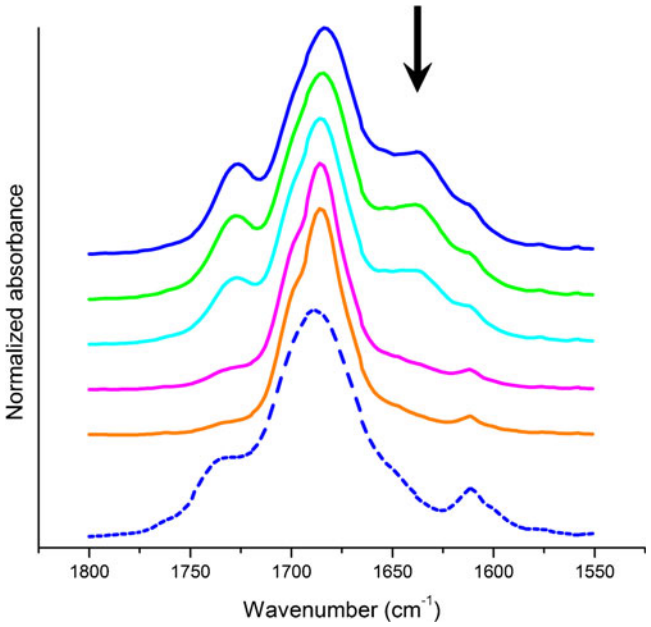

Fig. 8. Infrared spectra of the carbonyl region of indoprofen–PVP solid dispersion samples containing (*top to bottom*): (*solid blue*) 50% (*w/w*) API immediately after formation, and following storage at (*solid green*) 54, (*solid cyan*) 75, (*solid magenta*) 84, and (*solid orange*) 94% relative humidity and subsequent drying. The samples stored at 84% and 94% RH were determined to have crystallized. The calculated spectrum of a physical mixture containing 50% pure amorphous API and pure PVP (*dashed blue*) is also included for comparison

These results again suggest moisture-induced amorphous–amorphous phase separation behavior for samples containing 50% or more PVP, limited effects for sample containing 30% PVP, and no effects for sample containing 10% PVP.

For the indoprofen–PVP system (Fig. 8), when the sample containing 50% (*w/w*) PVP was exposed to moisture at increasing relative humidity, a slight increase in the relative intensity of the peak centered at 1,682 cm^{-1} was observed following storage at 54% and 75% RH, indicating the formation of more free PVP carbonyl groups. At 75% or lower RH, no indication of API crystallization was observed, suggesting moisture-induced amorphous–amorphous phase separation in the system. An abrupt decrease in the peak at 1,641 cm^{-1}, assigned to the PVP carbonyl hydrogen bonded to the API was observed following storage at 84% and 94% RH. This can be explained by crystallization of the API, detected through the appearance of a sharp peak centered at 738 cm^{-1} in these samples. For the sample containing 30% PVP, a similar trend was again observed, but evidence of API crystallization was detected following storage at 75% RH. For the sample containing 10% PVP, evidence of API crystallization was detected after storage at 54% RH. Since this was the lowest RH that the ASD samples were stored in after preparation, definite conclusion on whether observed API crystallization was preceded by amorphous–amorphous phase separation cannot be made. For samples containing 70% and 90% PVP, evidence of moisture-induced amorphous–amorphous phase separation was observed, with no evidence of API crystallization after storage at RH as high as 94%.

For the nilutamide–PVP system, shown in Fig. 9, exposure of the sample containing 50% PVP to moisture at increasing relative humidity resulted in a gradual decrease in the relative intensity of the peak centered at 1,663 cm^{-1}.

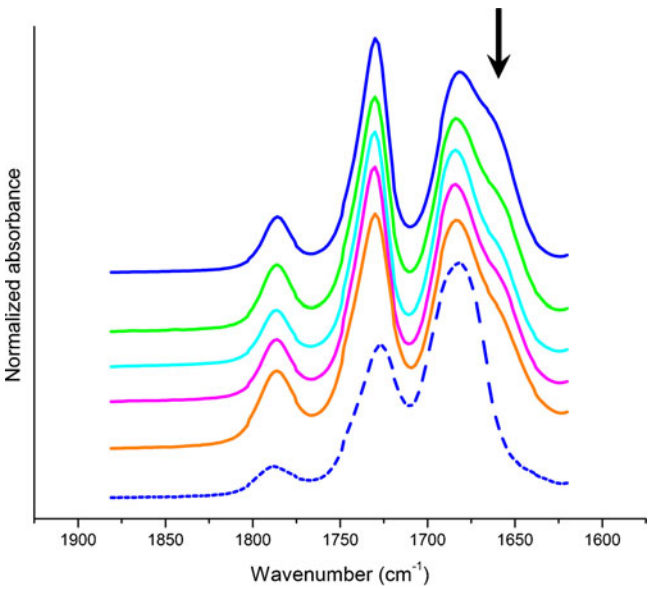

Fig. 9. Infrared spectra of the carbonyl region of nilutamide–PVP solid dispersion samples containing (*top to bottom*): (*solid blue*) 50% API immediately after formation, and following storage at (*solid green*) 54, (*solid cyan*) 75, (*solid magenta*) 84, and (*solid orange*) 94% relative humidity and subsequent drying. The calculated spectrum of a physical mixture containing 50% pure amorphous API and pure PVP (*dashed blue*) is also included for comparison

Concurrently, the relative intensity of the peak centered at 1,682 cm^{-1} gradually increased. Similar changes were also observed in samples containing 10%, 30%, 70%, and 90% (*w*/*w*) PVP (results not shown). In contrast to indoprofen–PVP system, spectroscopic evidence of the presence of crystalline nilutamide was not observed in any of the samples following storage at various RHs.

When loratadine–PVP samples containing 50% PVP were exposed to moisture at increasing relative humidity, the single peak initially centered at 1,686 cm^{-1} gradually separated into a peak centered at 1,692 cm^{-1} and a shoulder at 1,675 cm^{-1} as shown in Fig. 10. The separation of the single broad peak in the ASDs towards the carbonyl peaks of pure PVP and pure amorphous loratadine can be interpreted as evidence of moisture-induced amorphous–amorphous phase separation in the system. This conclusion is also supported by the fact that following storage at 94% RH and subsequent drying, the infrared spectrum of the sample became similar to the theoretically calculated spectra of a physical mixture sample containing 50% pure amorphous loratadine. Similar behavior was exhibited by samples containing 10%, 30%, 70%, and 90% PVP (results not shown).

The overall miscibility behavior of the different ASD samples investigated in this study is summarized in Table I.

DISCUSSION

In order to ensure the physical stability of an amorphous molecular-level solid dispersion, it is important to evaluate the extent of mixing between the API and the polymer not only immediately after production, but also following exposure to environmental stresses such as moisture. In particular, it is of interest to know whether the absorption of moisture by the system will result in the formation of amorphous API-rich and polymer-rich regions. This behavior is important to anticipate because the formation of an amorphous phase with API-rich and polymer-rich regions has been linked to accelerated API crystallization rates in a number of systems (3,15,16). In addition, any changes in the miscibility of an ASD can also potentially influence the dissolution behavior of the API.

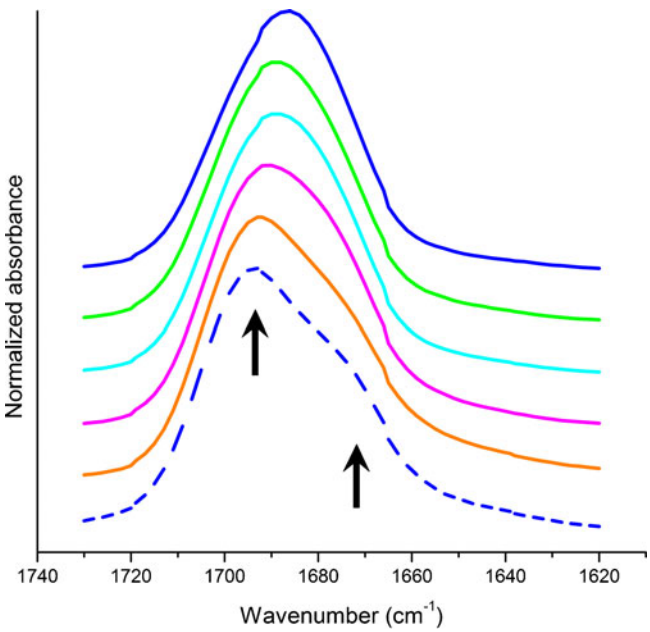

Fig. 10. Infrared spectra of the carbonyl region of loratadine–PVP solid dispersion samples containing (*top to bottom*): (*blue*) 50% API immediately after formation, and following storage at (*green*) 54, (*cyan*) 75, (*magenta*) 84, and (*orange*) 94% relative humidity and subsequent drying. The calculated spectrum of a physical mixture containing 50% pure amorphous API and pure PVP (*dashed blue*) is also included for comparison

To date, a total of 20 drug–polymer systems have been evaluated with respect to their tendency to undergo moisture-induced immiscibility. Table II summarizes potentially relevant physical properties pertaining to the different ASD systems investigated in this and previous studies. For each drug–polymer system, a category-based value has been assigned; for systems exhibiting moisture-induced amorphous–amorphous phase separation, a value of 0 was given, whereas for systems where this phenomenon was absent, a value of 1 was assigned.

Close examination of the table underlines the importance of the various factors that have been implicated in determining the phase behavior of ASDs containing a hydrophobic API following exposure to moisture: hygroscopicity of the ASD system (6), hydrophobicity of the API (7), and the strength of API–polymer interactions (7,8,17). Hence, previous studies have shown that ASDs prepared with a less hygroscopic polymers, for example HPMCAS, are in general, less susceptible to moisture induced amorphous–amorphous phase separation (3). In contrast, ASDs formed with PVP, an extremely hygroscopic polymer, appear to be highly vulnerable to this phenomenon, although Table II suggests that the susceptibility is highly dependent on the specific API used. Therefore, one focus of the current study has been to try and better understand the effects of moisture on the phase behavior of PVP-containing dispersions, given the widespread use of this polymer in dispersions (18,19). The strength of drug–polymer interactions has been highlighted as one of the key features determining the phase behavior of PVP containing ASDs, and the model compounds studied herein provide a broad range of hydrogen-bonding interactions with PVP and, together with previously studied drug–PVP systems, allow further probing of the role of drug–polymer hydrogen bonding.

The strength of API–polymer interactions are represented in Table II through two properties: the pK_a values of the API (when the hydrogen atom in the molecule is acting as a donor in hydrogen-bond type of interaction), and the extent of the red shift observed with the carbonyl peak of PVP in the binary systems. pK_a is a quantitative measure of the strength of an acid in solution. A compound with a lower pK_a value is considered as a stronger acid, whereby dissociation of the hydrogen atom from the molecules of such compounds in an aqueous environment is easier. Such a compound would be expected to be a better donor in a hydrogen-bonding interaction. The strength of the interaction can also be probed using infrared spectroscopy (7,20,21). When a compound containing a stronger hydrogen-bond donor is combined with a common hydrogen-bond acceptor, for example, the CO moiety in PVP, a larger red shift in the infrared peak can be expected than for compounds with weaker donors

Table II. Selected Physical Properties of Binary Amorphous Solid Dispersion Systems Evaluated in This and Other Published Studies

	API properties												PVP carbonyl shift in solid dispersion IR (cm^{-1})	ASD system phase behavior[g]
System	Molar mass (g/mol)[a]	No. of H-bond donor per molecule[b]	H-bond donor type	pK_a[l]	No. of H-bond acceptor[b]	H-bond acceptor type	log P[d]	log S[e]	T_g[f] (K)	ΔC_p[f] (J/molK)	T_m[k] (K)	ΔH_f[k] (kJ/mol)		
Indomethacin PVP	357.8	1	COOH	4.5[c]	4	N, O	3.58	−4.554	320.7	0.41	432[h]	38[h]	42	1
Indomethacin PVPVA	357.8	1	COOH	4.5[c]	4	N, O	3.58	−4.554	320.7	0.41	432[h]	38[h]	N/A	1
Indomethacin HPMAS	357.8	1	COOH	4.5[c]	4	N, O	3.58	−4.554	320.7	0.41	432[h]	38[h]	N/A	1
Ketoprofen PVP	254.3	1	COOH	5.02[i]	3	CO	3.31	−3.248	319.8	0.40	367[h]	27.2[h]	44	1
Indoprofen PVP	281.3	1	COOH	5.8[c]	3	CO, N	2.84	−4.824	323.2	N/A	485	36	41	0
Clofoctol PVP	365.3	1	OH	10.28	1	O	8.19	N/A	270.7	0.64	361	35.2	18	0
Probucol PVP	516.8	2	OH	10.59	2	O	10.0	−8.412	301.2	N/A	400	34.2	15	0
Quinidine PVP	324.4	1	OH	13.89	4	N, O	2.48	−2.812	334	0.59	444	35.2	19	0
Quinidine PVPVA	324.4	1	OH	13.89	4	N, O	2.48	−2.812	334	0.59	444	35.2	19	0
Quinidine HPMAS	324.4	1	OH	13.89	4	N, O	2.48	−2.812	334	0.59	444	35.2	19	1
Droperidol PVP	379.4	1	NH	12.72	4	N, O, F	1.92	−4.966	307	0.48	417[h]	44.9[h]	24	0
Pimozide PVP	461.6	1	NH	12.9	4	N, O, F	5.34	−5.202	335.5	0.42	491[h]	46[h]	20	0
Pimozide PVPVA	461.6	1	NH	12.9	4	N, O, F	5.34	−5.202	335.5	0.42	491[h]	46[h]	N/A	0
Pimozide HPMAS	461.6	1	NH	12.9	4	N, O, F	5.34	−5.202	335.5	0.42	491[h]	46[h]	N/A	1
Felodipine PVP	384.3	1	NH	28.18	5	N, O	2.24	−5.153[j]	320.2	0.34	420	31	20	0
Felodipine PVPVA	384.3	1	NH	28.18	5	N, O	2.24	−5.153[j]	320.2	0.34	420	31	N/A	0
Felodipine HPMAS	384.3	1	NH	28.18	5	N, O	2.24	−5.153[j]	320.2	0.34	420	31	N/A	1
Nifedipine PVP	346.3	1	NH	28.09	7	N, O	2.31	−3.948[j]	320.8	0.44	446	38.2	21	0
Nilutamide PVP	379.4	1	NH	15.01	7	N, O, F	2.14	N/A	308.4	0.41	428	31	18	0
Loratadine PVP	310.8	0	None	N/A	3	N, O	4.13	−5.063	312.4	0.33	409	27.3	−17	0

F is included as an H-bond donor, although it is not commonly involved in hydrogen-bonding interactions (23)

[a] Values obtained from reference (24)

[b] Values cited from PubChem BioAssay database, http://pubchem.ncbi.nlm.nih.gov

[c] Values obtained from reference (25)

[d] Values estimated using ChemBioDraw Ultra v 11.0, CambridgeSoft Corp., Cambridge, Massachusetts, USA

[e] Values obtained from reference (26) unless otherwise indicated

[f] Values obtained by heating a sample of crystalline API approximately 10 K above its melting temperature, cooling the sample to 253 K at >20 K/min, then re-heating the sample at 20 K/min using a calibrated Q10 or Q2000 DSC (TA Instruments, New Castle, Delaware, USA), as described in reference (7)

[g] Systems which did not exhibit amorphous–amorphous phase separation upon exposure to moisture are assigned a value of 1, while systems undergoing moisture-induced amorphous–amorphous phase separation were assigned a value 0

[h] Values obtained from reference (7)

[i] Value adopted from reference (27)

[j] Value adopted from reference (4)

[k] Values adopted from reference (28) unless otherwise indicated

[l] Values calculated using MarvinSketch Applet, ChemAxon Kft, Budapest, Hungary, http://www.chemaxon.com, unless otherwise indicated

(higher pK_a values). The strength of the hydrogen-bond donor will be dictated by the electronegativity of the bonding atom as well as the presence of any electron-withdrawing substituents. As seen from Table II, the compounds tend to form two groups, with the carboxylic acid-containing compounds resulting in larger red shifts in the PVP carbonyl (>40 cm^{-1}) than the hydroxyl and NH-containing compounds (around 15–20 cm^{-1}). Interestingly, with the exception of indoprofen, there is an excellent correlation between the extent of the PVP carbonyl red shift and the tendency of the system to undergo amorphous–amorphous phase separation. For the indoprofen ASDs, a small extent of phase separation was observed, and this observation can most likely be rationalized by consideration of the indoprofen pK_a shown in Table II—based on this value, indoprofen is clearly a somewhat weaker acid than the other carboxylic acids studied.

The lack of moisture-induced amorphous–amorphous phase separation observed for high drug loadings in the clofoctol–PVP and probucol–PVP dispersions also requires further comment, since at first glance these particular systems appear to be outliers. The *log P* values are reported to be 8.19 and 10.0 for clofoctol and probucol, respectively (see Table II), indicating high inherent hydrophobicity. Based on previous observations, very hydrophobic compounds which do not form extremely strong interactions with the polymer, have been found to undergo moisture-induced amorphous–amorphous phase separation (7). From the IR data shown above, it can be inferred that these compounds can form moderate interactions with PVP, as expected for phenolic hydrogen-bond donors. Amorphous–amorphous phase separation following exposure to moisture was indeed seen for some drug–polymer ratios, as summarized in Table I. However, at high drug loadings, it is thought that insufficient moisture is sorbed by the systems as a result of the extremely hydrophobic nature of the drugs. Hence, for clofoctol–PVP dispersions containing 70% (*w*/*w*) API or more and the probucol–PVP system containing 90% (*w*/*w*) API, exposure to moisture at RHs as high as 94% RH did not result in the formation of API-rich and polymer-rich amorphous regions, as evidenced by the persistence of the API–polymer interactions when probed using infrared spectroscopy. Other less hydrophobic model compounds that also form weak or moderate interactions, in contrast, were observed to undergo moisture-induced phase separation for all drug–polymer concentrations. In loratadine–PVP binary systems, the API and the polymer can only interact through weak C–H hydrogen bonding or dipole–dipole type of interactions. Moisture-induced amorphous–amorphous phase separation behavior was indeed observed for this drug–polymer combination throughout different drug–polymer ratios, as expected. Nilutamide contains a moderate strength hydrogen-bond donor, namely a NH moiety and as expected, forms a hydrogen bond with the carbonyl group of PVP (see Fig. 9). However, similar to other model APIs with NH-type hydrogen-bond donors (5,7), this system exhibits moisture-induced amorphous–amorphous phase separation with PVP at all drug–polymer ratios investigated. These observations highlight the complexity of this phenomenon and the need to consider not only drug and polymer properties, but also the relative proportions of each component.

The data presented in Table II was further analyzed by constructing an OPLS-DA model in order to better understand the properties of ASD systems resistant to moisture-induced amorphous–amorphous phase separation. As previously mentioned, an OPLS-DA model consists of one predictive component as well as any number of orthogonal components explaining within-class variability. Hence, in this case, the predictive component describes the system descriptors important for the absence of moisture-induced amorphous–amorphous phase separation. The OPLS-DA model constructed using the data in Table II resulted in one predictive component as well as two orthogonal components with a goodness of fit (R^2Y) of 0.98 and goodness of prediction (Q^2) of 0.73, indicative of a good model (22). The number of hydrogen-bond acceptors and donors, as well as *MW*, *log P*, *log S*, and T_g were excluded from the model, since these variables made insignificant contributions to the model. The type of hydrogen-bond donor and acceptors were evaluated as qualitative variables in the model.

The predictive component of the OPLS-DA model (Fig. 11) shows that a decrease in the pK_a of the API as well as an increase in the PVP carbonyl red shift will lead to a system that does not undergo moisture-induced changes in miscibility, as discussed above. In addition, a lower ΔC_p value of the pure amorphous API is also a property common to these ASD systems, although the underlying basis for this observation is, at present, unknown. The presence of a COOH hydrogen-bond donor moiety in the API is also indicative of an ASD system that remains miscible on exposure to moisture, whereas the presence of NH and OH groups results in a tendency to undergo moisture-induced amorphous–amorphous phase separation. A lone CO hydrogen-bond acceptor group in the API is also indicative of a non-phase separating system, whereas the presence of an F atom seems to contribute towards a tendency for moisture-induced phase separation, and it can be speculated that this is due to its effect on the hydrophobicity of the molecule (23).

From the chemometrics analysis, the orthogonal components (Fig. 12) of the model describe the intra-class difference between systems not exhibiting moisture-induced amorphous–amorphous phase separation (dashed lines) as well as systems exhibiting this phenomenon (dotted lines); while the predictive component explains what variables distinguish the two classes of systems, there are other variations in the data set that are important in order to accurately predict the phase behavior of a system. This orthogonal variation requires two components to be added to the model (the predictive component is always altered with the addition of an orthogonal component). When assessing the score plot of these components (Fig. 12), it is evident that the two orthogonal components describe the intra-class difference between the different systems. If these systems were completely orthogonal to each other, then, each orthogonal component would describe the difference within each system. However, this is not the case. In addition, the indoprofen–PVP system is found to not belong to either system; in other words, it is an outlier within the property space of these systems. It has many features associated with systems not exhibiting amorphous–amorphous phase separation, but also possesses key properties of systems exhibiting such behavior. Filtering this out of the predictive component not only makes

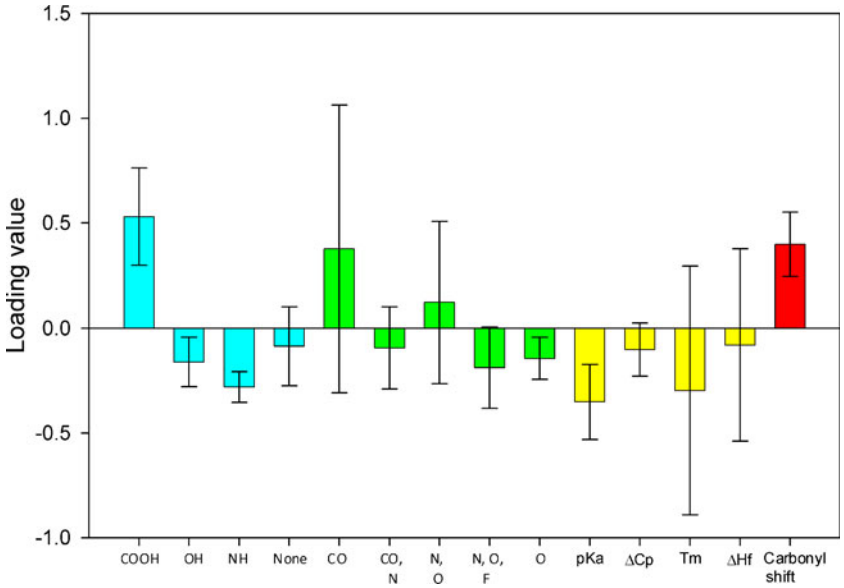

Fig. 11. Loadings of the predictive component of the OPLS-DA model constructed from the dataset. *Blue bars* represent H-bond donors, *green bars* represent H-bond acceptors, *yellow bars* represent properties of the drug, and the *red bar* represents the PVP carbonyl red shift observed using infrared spectroscopy. Tendency to avoid moisture induced amorphous-amorphous phase separation is improved if a carboxylic acid H-bond donor group is present and when a strong PVP carbonyl shift is noticed, indicative of an interaction with PVP. Lower API pK_a is also more likely to form a system resistance to amorphous phase separation according to the model

the predictive component interpretable in terms of phase separation tendency, but it also improves the model. The outlier characteristics of the indoprofen–PVP model system can be seen in Fig. 12. Although it shares many features of a system not exhibiting amorphous–amorphous phase separation, it still does not fit that class in the model because of the presence of both CO and NH bond acceptors. The missing value for ΔC_p for pure amorphous indoprofen system may be a reason for the significance of this factor (this value could not be easily obtained experimentally because indoprofen is a rapid crystallizer). This outlier characteristic of indoprofen–PVP can be further understood from the experimental results, where evidence for the formation of API-rich and polymer-rich regions was observed, but not at the expense of a complete removal of API–polymer strong specific interactions as exhibited by some presence of a shift in the IR peak assigned to PVP following storage at 54% and 75% RH for the sample containing 50% (*w*/*w*) PVP. Thus, indoprofen seems to be an example of a carboxylic acid containing compound that can undergo a small extent of phase separation when exposed to moisture.

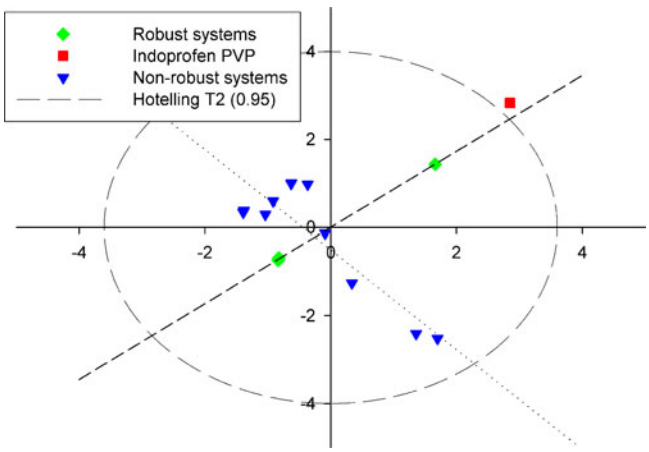

Fig. 12. Score plot of orthogonal components illustrating the outlying properties of the indoprofen–PVP system (*red square*). *Green diamonds* represent the three systems which remain miscible in the presence of moisture, while *blue triangles* represent the systems that undergo amorphous phase separation on exposure to moisture. The *Hotelling's T2 line* represents the boundary of similarity, thus illustrating the outlier characteristics of the indoprofen–PVP model system; indoprofen–PVP has similar properties to the miscible systems, but is still outside their property space, which confirms its tendency to undergo moisture-induced phase separation

CONCLUSIONS

In this study, component miscibility and phase behavior of different amorphous molecular-level solid dispersions following absorption of moisture at different relative humidities was studied and patterns of behavior were analyzed by taking into consideration various physicochemical properties. The following characteristics appear to result in systems exhibiting a propensity to resist amorphous–amorphous phase separation upon exposure to atmospheric moisture: (1) minimal hygroscopicity of the ASD (which in turn depends on the hygroscopicity of the polymer and the API, the strength of interactions between the two components and, of course, the RH), (2) a less hydrophobic API, and (3) the strength of API–polymer interactions. The results obtained in this study will aid in the design of more stable ASDs and appropriate accelerated stability testing regimes.

ACKNOWLEDGMENTS

Matthew J. Jackson is gratefully acknowledged for his help in collecting infrared results. This work is funded by Purdue Research Foundation and Merck Research Laboratories. This work was supported in part by a grant from the Lilly Endowment, Inc., to Purdue University School of Pharmacy and Pharmaceutical Sciences. BVE is a Postdoctoral Researcher of the 'Fonds voor Wetenschappelijk Onderzoek', Flanders, Belgium.

REFERENCES

1. Hancock BC, Parks M. What is the true solubility advantage for amorphous pharmaceuticals? Pharm Res. 2000;17(4):397–404.
2. Konno H, Taylor LS. Ability of different polymers to inhibit the crystallization of amorphous felodipine in the presence of moisture. Pharm Res. 2008;25(4):969–78.
3. Rumondor ACF, Stanford LA, Taylor LS. Effects of polymer type and storage relative humidity on the kinetics of felodipine crystallization from amorphous solid dispersions. Pharm Res. 2009;26(12):2599–606.
4. Marsac PJ, Konno H, Rumondor ACF, Taylor LS. Recrystallization of nifedipine and felodipine from amorphous molecular level solid dispersions containing poly(vinylpyrrolidone) and sorbed water. Pharm Res. 2008;25(3):647–56.
5. Marsac PJ, Rumondor ACF, Nivens DE, Kestur US, Stanciu L, Taylor LS. Effect of temperature and moisture on the miscibility of amorphous dispersions of felodipine and poly(vinyl pyrrolidone). J Pharm Sci. 2010;99(1):169–85.
6. Rumondor ACF, Taylor LS. Effects of polymer hygroscopicity on the phase behavior of amorphous solid dispersions in the presence of moisture. Mol Pharm. 2010;7(2):477–90.
7. Rumondor ACF, Marsac PJ, Stanford LA, Taylor LS. Phase behavior of poly(vinylpyrrolidone) containing amorphous solid dispersions in the presence of moisture. Mol Pharm. 2009;6 (5):1492–505.
8. Vasanthavada M, Tong WQ, Joshi Y, Kislalioglu MS. Phase behavior of amorphous molecular dispersions-II: role of hydrogen bonding in solid solubility and phase separation kinetics. Pharm Res. 2005;22(3):440–8.
9. Rumondor ACF, Konno H, Marsac P, Taylor L. Analysis of the moisture sorption behavior of amorphous solid dispersions containing hydrophobic drugs. J Appl Polymer Sci. 2010;117(2):1055–63.
10. Bylesjö M, Rantalainen M, Cloarec O, Nicholson JK, Holmes E, Trygg J. OPLS discriminant analysis: combining the strengths of PLS-DA and SIMCA classification. J Chemometr. 2006;20:341–51.
11. Rumondor ACF, Ivanisevic I, Bates S, Alonzo DE, Taylor LS. Evaluation of drug-polymer miscibility in amorphous solid dispersion systems. Pharm Res. 2009;26(11):2523–34.
12. Broman E, Khoo C, Taylor LS. A comparison of alternative polymer excipients and processing methods for making solid dispersions of a poorly water soluble drug. Int J Pharm. 2001;222 (1):139–51.
13. Taylor LS, Zografi G. Spectroscopic characterization of interactions between PVP and indomethacin in amorphous molecular dispersions. Pharm Res. 1997;14(12):1691–8.
14. Allen FH. The Cambridge Structural Database: a quarter of a million crystal structures and rising. Acta Cryst. 2002;B58:380–8.
15. Qian F, Huang J, Zhu Q, Haddadin R, Gawel J, Garmise R, *et al.* Is a distinctive single T_g a reliable indicator for the homogeneity of amorphous solid dispersion? Int J Pharm. 2010;395(1–2):232–5.
16. Ivanisevic I. Physical stability studies of miscible amorphous solid dispersions. J Pharm Sci. 2010;99(9):4005–12.
17. Marsac P, Li T, Taylor L. Estimation of drug-polymer miscibility and solubility in amorphous solid dispersions using experimentally determined interaction parameters. Pharm Res. 2009;26(1):139–51.
18. Leuner C, Dressman J. Improving drug solubility for oral delivery using solid dispersions. Eur J Pharm Biopharm. 2000;50(1):47–60.
19. Serajuddin ATM. Solid dispersion of poorly water-soluble drugs: early promises, subsequent problems, and recent breakthroughs. J Pharm Sci. 1999;88(10):1058–66.
20. Tang XLC, Pikal MJ, Taylor LS. A spectroscopic investigation of hydrogen bond patterns in crystalline and amorphous phases in dihydropyridine calcium channel blockers. Pharm Res. 2002;19 (4):477–83.
21. Wolkers WF, Oliver AE, Tablin F, Crowe JH. A Fourier-transform infrared spectroscopy study of sugar glasses. Carbohydr Res. 2004;339(6):1077–85.
22. Eriksson L, Johansson E, Kettaneh-Wold N, J.Trygg, Wikström C, Wold S. Multivariate and Megavariate Data Analysis Basic Principles and Applications (Part I): Umetrics; 2006.
23. Laurence C, Brameld KA, Graton J, Le Questel JY, Renault E. The pK(BHX) database: toward a better understanding of hydrogen-bond basicity for medicinal chemists. J Med Chem. 2009;52(14):4073–86.
24. The Merck Index: An Encyclopedia of Chemicals, Drugs, and Biologicals. 14th ed. al. MJone, editor. Whitehouse Station, NJ: Merck & Co., Inc.; 2006.
25. Thompson JE. A Practical Guide to Contemporary Pharmacy Practice. 3rd ed. Baltimore: Lippincott Williams & Wilkins; 2009.
26. Yalkowsky SH, He Y. Handbook of Aqueous Solubility Data: CRC Press; 2003.
27. Chi SC, Jun HW. Release rates of ketoprofen from poloxamer gels in a membraneless diffusion cell. J Pharm Sci. 1991;80(3):280–3.
28. Baird JA, Van Eerdenbrugh B, Taylor LS. A classification system to assess the crystallization tendency of organic molecules from undercooled melts. J Pharm Sci. 2010;99(9):3787–806.